

Direct Observation of Local Potassium Variation and Its Correlation to Electronic Inhomogeneity in $(\text{Ba}_{1-x}\text{K}_x)\text{Fe}_2\text{As}_2$ Pnictide

W. K. Yeoh,^{1,*} B. Gault,^{1,2} X. Y. Cui,¹ C. Zhu,¹ M. P. Moody,¹ L. Li,¹ R. K. Zheng,^{1,†} W. X. Li,³ X. L. Wang,³ S. X. Dou,³ G. L. Sun,⁴ C. T. Lin,⁴ and S. P. Ringer¹

¹Australian Centre for Microscopy & Microanalysis, University of Sydney, Sydney, New South Wales 2006, Australia

²ANSTO, Institute of Materials Engineering, New Illawarra Road, Lucas Heights, New South Wales, Australia

³Institute for Superconducting & Electronic Materials, University of Wollongong, North Wollongong, New South Wales 2500, Australia

⁴Max-Planck-Institut für Festkörperforschung, Heisenbergstraße 1, D-70569 Stuttgart, Germany

(Received 28 February 2011; published 15 June 2011)

Local fluctuations in the distribution of dopant atoms are thought to cause the nanoscale electronic disorder or phase separation in pnictide superconductors. Atom probe tomography has enabled the first direct observations of dopant species clustering in a K-doped 122-phase pnictide. First-principles calculations suggest the coexistence of static magnetism and superconductivity on a lattice parameter length scale over a wide range of dopant concentrations. Our results provide evidence for a mixed scenario of phase coexistence and phase separation, depending on local dopant atom distributions.

DOI: 10.1103/PhysRevLett.106.247002

PACS numbers: 74.70.Xa, 36.40.-c, 74.25.Jb, 74.62.Bf

Since the discovery of the superconductivity in iron pnictide [1–3], the phase diagram has been a focus of intense research and debate due to the competition between the antiferromagnetic spin-density-wave (AFM-SDW) and the superconducting (SC) states. On the one hand, there is recent experimental evidence that magnetically ordered phases and SC states are microscopically separated [4–7], while on the other hand, there is evidence that these phases coexist (e.g.) [8–11] in the K or Co-doped BaFe_2As_2 (122-FeAs) system. So far, most studies on K or Co-doped materials are in favor of the coexistence of magnetic order and superconductivity [8–11], and have consistently ruled out phase separation [12–14]. Conversely, Park *et al.* [4] have recently proposed an electronic phase separation of the AFM and SC states, and their model has been supported by others using muon spin relaxation [5], ⁷⁵As NMR [6] and neutron-diffraction measurements [7].

As the magnetism and SC evolve with the doping level, the coexistence or separation of these phases is likely to be correlated to local dopant atom distributions. However, the lack of direct experimental atomic scale evidence makes this question difficult to answer. Atom probe tomography (APT) [15,16] provides three-dimensional chemical mapping with near-atomic resolution and is ideally suited to investigate dopants distribution. Here, we apply APT to resolve the origins of the electronic disorder in 122-FeAs-based superconductors by posing the hypothesis that non-uniform dopant atom distributions induce changes to the T_c , and investigating whether the AFM and SC phases do, in fact, coexist.

$(\text{Ba}_{0.72}\text{K}_{0.28})\text{Fe}_2\text{As}_2$ crystals were obtained by the self-flux method [17]. A superconducting transition temperature T_c occurred at 32 K for the doped $\text{Ba}_{0.75}\text{K}_{0.25}\text{Fe}_2\text{As}_2$ [18], in agreement with Ref. [19]. The specific heat was

measured from 1.9 to 305 K at zero field and 12 T, using a long relaxation technique [20]. Needle-shaped atom probe specimens with tip radius of <100 nm were prepared by focused ion beam (FIB) on dual beam instruments (FEI Quanta 200 and xT Nova NanoLab 200) as described in Ref. [21]. After annular FIB milling, specimens were cleaned using low energy ion milling to minimize Ga implantation. Pulsed-laser APT analyses were performed on a LEAP 3000X Si (Cameca Corp.), with a flight length of 90 mm, at a base pressure of 3×10^{-11} torr, a temperature of 20 K, a laser pulse energy of 0.2 nJ (wavelength $\lambda = 532$ nm), focused to a spot of diameter <10 μm , and at a repetition rate of 200 kHz.

Figure 1(a) presents an APT reconstruction of K-doped BaFe_2As_2 superconductor, generated from a data set of $>10^6$ atoms with the Fe, As, Ba, and K atoms displayed. Single atoms are represented by dots, and the dot color indicates the chemical identity as determined by AP time-of-flight mass spectroscopy. The measured Ba:K:Fe:As ratio within the reconstruction was 1.92:0.68:3.7:3.7, close to the expected 1.5:0.5:4:4. It is noteworthy that the 1:1 ratio of Fe and As and 3:1 for Ba and K are preserved. Enlarged section of Ba and K lattice planes along the (001) pole, oriented perpendicular to the growth direction is presented in Fig. 1(b). Structural information can be obtained by means of spatial distribution maps (SDM) [22], effectively a 1D radial distribution function, along the reconstructed (001) direction. A spatial distribution histogram of Ba and K atoms relative to Fe atoms in the c axis is plotted in Fig. 1(c). Three obvious peaks corresponding to interspacing values of 1.15, 2.2, and 3.8 nm can be detected within a 4 nm distance, with Fe planes serving as the reference planes. This value agrees closely with the expected value of lattice plane spacing in this direction between Fe and its nearest Ba/K neighbors. The overlap

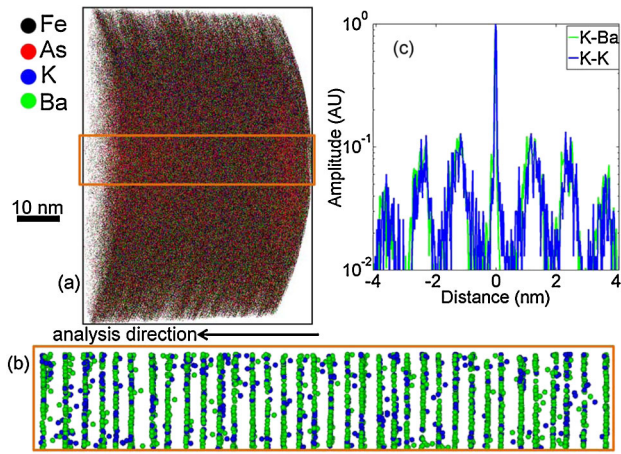


FIG. 1 (color online). (a) 3D APT reconstruction of $(\text{Ba}_{0.72}\text{K}_{0.28})\text{Fe}_2\text{As}_2$, superconductor. Each dot represents individual atom of K, Ba, As, and Fe (b) Subvolume from (a) showing atomic lattice planes of K and Ba. Spacing between each plane is $c/2$ (c) 1D spatial distribution maps in the analysis direction highlights the distribution of K and Ba in atomic planes.

between their peak in the SDM analysis also confirms that B and K reside in the same plane, at $c/2$.

The nanoscale distribution of K and Ba was investigated using a frequency distribution analysis, whereby the K and Ba compositions were determined in blocks of 100 atoms within the data, as shown in Fig. 2. Each frequency distribution was compared directly to the corresponding binomial distribution expected if the solutes were distributed randomly. The histogram peaks indicate that Ba and K have the average concentration of 0.12 and 0.05 wt %, respectively, which are close to their nominal concentra-

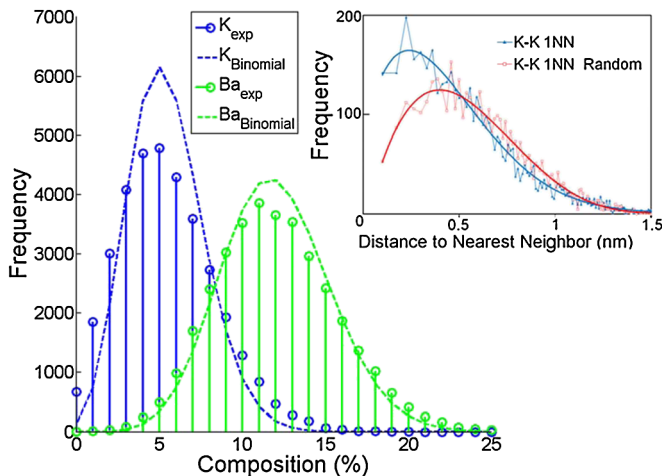


FIG. 2 (color online). Frequency distribution of Ba and K atoms. The dashed line shows the binomial distribution expected for a random distribution. (Inset) Nearest neighbor distribution of K for the experimental data and also the randomized case. The solid line is the fitting result for both distributions.

tions. The K frequency distribution was found to have considerable deviation from the binomial distribution with χ^2 test value ($\chi^2 = 629.24$ for 15 degrees of freedom) implying a significantly nonuniform distribution. The Ba frequency distribution was closer to the expected binomial distribution, with a χ^2 test value ($\chi^2 = 69.53$ for 23 degrees of freedom) indicating a more homogeneous distribution. Nearest neighbor (NN) analyses [23] are histograms examining the distribution of distances separating a solute atom from its nearest solute atom neighbor. There is a clear shift to the left of the experimental K NN distribution, presented in the inset of Fig. 2, relative to that expected if the K atoms were randomly distributed. This indicates that there are significantly more than expected K atoms separated by small interatomic distances. These results strongly support the suggestion that K atoms in the 122 pnictide superconductor are not randomly distributed—rather, these atoms are clustered in a way that produces local nanoscale regions of both low and high K concentration.

The localized K content fluctuation in BaFe_2As_2 matrix will lead to inhomogeneous superconducting transitions and T_c fluctuations, which can be evaluated by a T_c distribution. As proposed by Wang *et al.* [24], the overall T_c distribution across a sample can be estimated from the specific heat measurements by means of a deconvolution method: $F(T) = \int_0^T f(T_c) dT_c$, where $F(T)$ is the integral of the distribution function, $f(T_c)$, and $F(T)$ represents the fraction in the sample with $T_c \leq T$ with the boundary condition of $F(T_{c,\text{max}}) = 1$. Figure 3 shows the $F(T)$ and $f(T_c)$ dependences on T for $(\text{Ba}_{0.72}\text{K}_{0.28})\text{Fe}_2\text{As}_2$ crystals. The superconducting transition starts at 32.5 K and reaches maximum value of 31 K followed by a slow decrease down to 17 K. The broad transition of 15 K is consistent with the influence of local fluctuations in the K

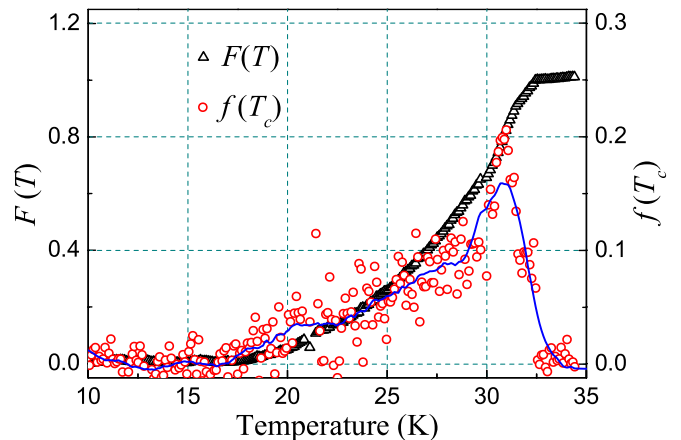


FIG. 3 (color online). T_c distribution in K-doped BaFe_2As_2 single crystals, obtained by deconvolution of the calorimetric data. The broader T_c distribution is due to the inhomogeneous K distribution.

TABLE I. Lattice constants and atomic magnetic moments of undoped and K-underdoped BaFe_2As_2 obtained from DFT-LDA.

Configurations	a, b, c (Å)	Magnetic moments (μ_B)
Pure	5.556, 5.503, 12.039	± 0.47
pure (exp) [28]	5.616, 5.571, 12.943	± 0.87 [28] or ± 0.99 [29]
Single <i>A</i>	5.461, 5.440, 12.171	± 0.344
Single <i>B</i>	5.455, 5.454, 12.285	$\pm 0.468, \pm 0.012, \pm 0.449, \pm 0.267$
Pair	5.398, 5.376, 12.568	0.708, -0.706
Trio	5.345, 5.239, 12.703	0.065, -0.647

concentration in the superconducting phases. Recent heat capacity measurements also suggest the presence of nanoscale inhomogeneity in the Co-doped BaFe_2As_2 system [25].

To understand how the K distributions impact the superconducting and magnetic properties, we performed extensive density-functional theory (DFT) calculations using the local-density approximation (LDA) [26] for the exchange-correlation functional, via the DMOL3 code [27]. A double numerical quality localized basis set, with a real-space cutoff of 11 bohr and Monkhorst-Pack grids of $8 \times 8 \times 4$ with 75 **k** points in the irreducible part of the Brillouin zone for the 20-atom cell were employed. Polarization functions and scalar-relativistic corrections were incorporated explicitly. For the doped systems, we deliberately enforce no symmetry constraints. The low-temperature orthorhombic F_{mmm} structure containing 0, 1, 2, and 3 K atoms substituting at the Ba atom sites, respectively, was employed to simulate the different solute regions. Full relaxation, including the atomic positions and lattice constants, was performed in all calculations.

The optimized structural data as well as the Fe-atomic magnetic moment are summarized in Table I. The magnetic structures of undoped and underdoped systems are

presented in Fig. 4. In agreement with other experiments [10], our first-principles calculations reveal that replacing Ba^{2+} with K^+ results in a continuous increase in c , and a decrease in a and b . For the pure BaFe_2As_2 , the magnetic structure is ferromagnetic along b and antiferromagnetic along a and c [30], with the calculated moment being $0.47\mu_B$, compared with the experimental values of $0.99\mu_B$ [29] and $0.87\mu_B$ [28]. Most of this underestimation is due to LDA. For instance, using experimental lattice constants, LDA predicts the Fe moment to be $0.68\mu_B$, while the generalized gradient approximation yields $1.98\mu_B$. For the underdoped systems, importantly, we found that there is finite magnetism in all dopant concentrations under LDA. The magnetic properties are extremely sensitive to the local symmetry and the atomic environment around dopants. For the trio and distorted single-*B* configurations (energetically degenerate to single *A*), atomic moment suppression occurs for only a fraction of the Fe atoms. While the underlying mechanisms of the competition or coexistence model are not well understood at the atomic level, ^{57}Fe -Mössbauer measurements indicate microscopic coexistence of the SDW and superconducting states [12]. Considering the fact that LDA-DFT generally underestimates magnetism, our results suggest that the

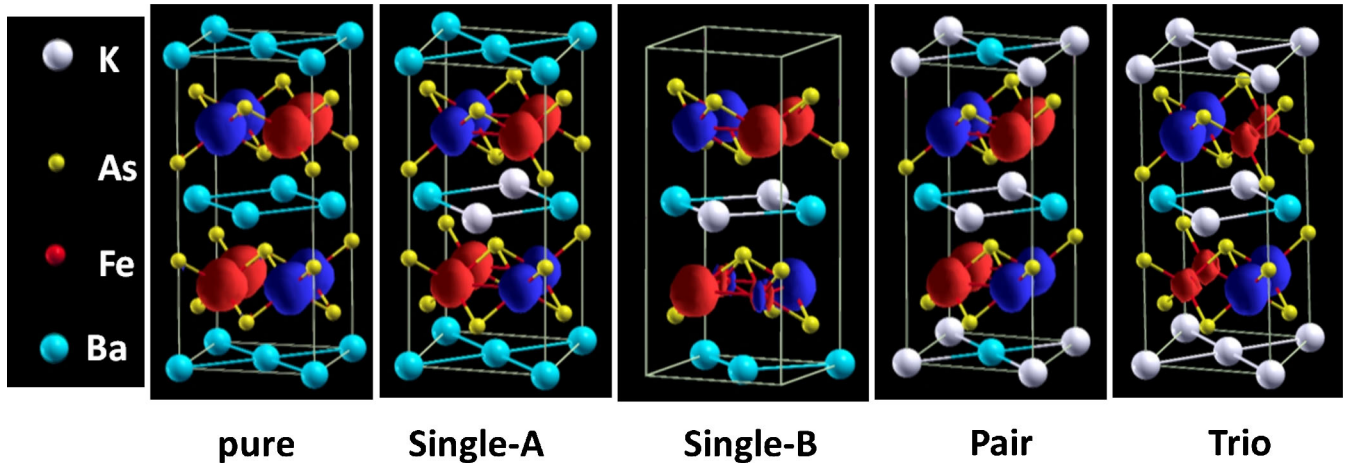


FIG. 4 (color online). Isosurface plots of the spin density of the pure and various K-underdoped BaFe_2As_2 based on LDA-DFT. Note the symmetry distortion after K doping and the nearly complete magnetism-suppression at a fraction of the Fe atoms in the single-*B* and trio structures. Red (light color) or blue (dark color) isosurfaces denote positive or negative spin polarization, respectively. The isosurface value is 0.02 electrons/ Å^3 .

complete suppression of magnetism is unlikely to occur in mesoscopic regions; rather, the AFM-SDW and SC are likely to coexist in an intimate nanoscale partitioning. This scenario is strongly supported by recent NMR investigations, showing that these two states coexist microscopically in underdoped compositions, over lattice parameter length scales [9,31]. The coexistence of superconductivity and incommensurate magnetic order has been proposed theoretically [32] and demonstrated in Co-doped BaFe_2As_2 [33].

Most superconductor studies make the assumption that the introduced carriers or dopants are distributed uniformly, leading to an expectation that these materials are electronically homogeneous. However, the present research challenges this assumption—via unequivocal evidence of clustering of K dopant atoms. Substitution of K atoms to the Ba sites has two major influences in the 122 system: suppression of the local Fe magnetism, and providing hole carriers to promote superconductivity. The inhomogeneity in K atom distribution manifests as spatial variations in both the local density of states spectra, and the superconducting energy gap, which separates the electron systems into hole-rich and hole-poor regions. This resembles the nanoscale superconducting gap variations observed in [13,34] where Masee *et al.* [13] correlated nanometer-sized regions with different gap magnitudes to that expected for the Co—Co interatomic separation. According to the K-doping phase diagram [2], the AFM-SDW state is absent in the high K-solute regions (overdoped), creating an exclusively SC state, whereas the coexistence of AFM and SC states occurs in the low K (underdoped) regions. Regions with no K only have a AFM state. Our experimental observations demonstrate the presence of atom clusters, which promote the coexistence of the AFM and SC states in what is effectively a K-concentration dependent nanoscale partitioning of the two phases. These observations are in agreement with Refs. [9,10,14,35] that all suggest that an inhomogeneous K concentration underpins disorder in the K-doped 122 compound. This situation resembles the much-discussed high T_c cuprate superconductor, where the oxygen distributions are strongly correlated to nanoscale electronic disorder and electronic phase segregation [36–38]. Similar phenomena are likely to be common in all the pnictides systems, where clustering of dopants may play a critical role on the local electronic disorder.

In summary, a combination of APT, T_c variations measurements and DFT simulations has been used to investigate the underlying cause of nanoscale electronic state variations and the coexistence of the AFM and SC states in K-doped superconductors. APT results indicate direct experimental evidence that the K atoms are not uniformly distributed in $(\text{Ba}_{1-x}\text{K}_x)\text{Fe}_2\text{As}_2$ pnictide and this was correlated to a broad T_c variation. DFT calculations indicate that the AFM and SC states may coexist on a lattice

parameter length scale. The competition between the AFM and SC states is highly sensitive to variations in the nanoscale microstructure. Variations of K atom distribution enable the coexistence of AFM and SC phases leading to highly localized electronic inhomogeneities.

This work is supported in part by the Australian Research Council. The authors acknowledge technical support from Dr. C.H. Kong of Electron Microscope Unit, University of New South Wales and the AMMRF at the University of Sydney, and particularly Dr. L. Stephenson and Ms. A. Ceguerra for helpful discussions.

*waikong.yeoh@sydney.edu.au

†rongkun.zheng@sydney.edu.au

- [1] J. Zhao *et al.*, *Nature Mater.* **7**, 953 (2008).
- [2] H. Chen *et al.*, *Europhys. Lett.* **85**, 17006 (2009).
- [3] H. Luetkens *et al.*, *Nature Mater.* **8**, 305 (2009).
- [4] J. T. Park *et al.*, *Phys. Rev. Lett.* **102**, 117006 (2009).
- [5] T. Goko *et al.*, *Phys. Rev. B* **80**, 024508 (2009).
- [6] H. Fukazawa *et al.*, *J. Phys. Soc. Jpn.* **78**, 033704 (2009).
- [7] D. S. Inosov *et al.*, *Phys. Rev. B* **79**, 224503 (2009).
- [8] A. A. Aczel *et al.*, *Phys. Rev. B* **78**, 214503 (2008).
- [9] M. H. Julien *et al.*, *Europhys. Lett.* **87**, 37001 (2009).
- [10] M. Rotter *et al.*, *New J. Phys.* **11**, 025014 (2009).
- [11] P. Marsik *et al.*, *Phys. Rev. Lett.* **105**, 057001 (2010).
- [12] F. L. Ning *et al.*, *J. Phys. Soc. Jpn.* **78**, 013711 (2009).
- [13] F. Masee *et al.*, *Phys. Rev. B* **79**, 220517 (2009).
- [14] D. Johrendt *et al.*, *Physica (Amsterdam)* **469C**, 332 (2009).
- [15] T. F. Kelly *et al.*, *Rev. Sci. Instrum.* **78**, 031101 (2007).
- [16] B. Gault *et al.*, *Ultramicroscopy* **111**, 448 (2011).
- [17] G. L. Sun *et al.*, *J. Supercond. Novel Magnetism* (in press).
- [18] X. L. Wang *et al.*, *Phys. Rev. B* **82**, 024525 (2010).
- [19] M. Rotter *et al.*, *Angew. Chem., Int. Ed.* **47**, 7949 (2008).
- [20] D. Sanchez *et al.*, *Physica (Amsterdam)* **200C**, 1 (1992).
- [21] P. Felfer *et al.*, *Ultramicroscopy* **111**, 435 (2011).
- [22] M. P. Moody *et al.*, *Ultramicroscopy* **109**, 815 (2009).
- [23] L. T. Stephenson *et al.*, *Microsc. Microanal.* **13**, 448 (2007).
- [24] Y. Wang *et al.*, *Supercond. Sci. Technol.* **19**, 263 (2006).
- [25] K. Gofryk *et al.*, *Phys. Rev. B* **81**, 184518 (2010).
- [26] J. P. Perdew *et al.*, *Phys. Rev. B* **45**, 13244 (1992).
- [27] B. Delley, *J. Chem. Phys.* **92**, 508 (1990); **113**, 7756 (2000).
- [28] Q. Huang *et al.*, *Phys. Rev. Lett.* **101**, 257003 (2008).
- [29] Y. Su *et al.*, *Phys. Rev. B* **79**, 064504 (2009).
- [30] E. Akturk *et al.*, *Phys. Rev. B* **79**, 184523 (2009).
- [31] R. R. Urbano *et al.*, *Phys. Rev. Lett.* **105**, 107001 (2010).
- [32] A. B. Vorontsov *et al.*, *Phys. Rev. B* **79**, 060508 (2009).
- [33] Y. Laplace *et al.*, *Phys. Rev. B* **80**, 140501 (2009).
- [34] Y. Yin *et al.*, *Phys. Rev. Lett.* **102**, 097002 (2009).
- [35] Y. Laplace *et al.*, *Eur. Phys. J. B* **73**, 161 (2010).
- [36] S. H. Pan *et al.*, *Nature (London)* **413**, 282 (2001).
- [37] K. McElroy *et al.*, *Science* **309**, 1048 (2005).
- [38] H. E. Mohottala *et al.*, *Nature Mater.* **5**, 377 (2006).